Near-Surface Plasma Characterization of the 12.5-kW NASA TDU1 Hall Thruster

Rohit Shastry[1], Wensheng Huang[2] and Hani Kamhawi[3]
NASA Glenn Research Center, Cleveland, OH, 44135

To advance the state-of-the-art in Hall thruster technology, NASA is developing a 12.5-kW, high-specific-impulse, high-throughput thruster for the Solar Electric Propulsion Technology Demonstration Mission. In order to meet the demanding lifetime requirements of potential missions such as the Asteroid Redirect Robotic Mission, magnetic shielding was incorporated into the thruster design. Two units of the resulting thruster, called the Hall Effect Rocket with Magnetic Shielding (HERMeS), were fabricated and are presently being characterized. The first of these units, designated the Technology Development Unit 1 (TDU1), has undergone extensive performance and thermal characterization at NASA Glenn Research Center. A preliminary lifetime assessment was conducted by characterizing the degree of magnetic shielding within the thruster. This characterization was accomplished by placing eight flush-mounted Langmuir probes within each discharge channel wall and measuring the local plasma potential and electron temperature at various axial locations. Measured properties indicate a high degree of magnetic shielding across the throttle table, with plasma potential variations along each channel wall being ≤ 5 V and electron temperatures being maintained at ≤ 5 eV, even at 800 V discharge voltage near the thruster exit plane. These properties indicate that ion impact energies within the HERMeS will not exceed 26 eV, which is below the expected sputtering threshold energy for boron nitride. Parametric studies that varied the facility backpressure and magnetic field strength at 300 V, 9.4 kW, illustrate that the plasma potential and electron temperature are insensitive to these parameters, with shielding being maintained at facility pressures 3X higher and magnetic field strengths 2.5X higher than nominal conditions. Overall, the preliminary lifetime assessment indicates a high degree of shielding within the HERMeS TDU1, effectively mitigating discharge channel erosion as a life-limiting mechanism.

Nomenclature

ARRM	=	Asteroid Redirect Robotic Mission
B_{max}	=	maximum radial magnetic field strength along channel centerline
GRC	=	Glenn Research Center
HERMeS	=	Hall Effect Rocket with Magnetic Shielding
JPL	=	Jet Propulsion Laboratory
n_e	=	electron number density
P_d	=	discharge power
SEP TDM	=	Solar Electric Propulsion Technology Demonstration Mission
T	=	thrust
T_e	=	electron temperature
TDU	=	Technology Development Unit
η_a	=	anode efficiency
ϕ_p	=	plasma potential

[1] Research Engineer, Electric Propulsion Systems Branch, 21000 Brookpark Rd., MS 301-3, AIAA Member.
[2] Research Engineer, Electric Propulsion Systems Branch, 21000 Brookpark Rd., MS 301-3, AIAA Senior Member.
[3] Research Engineer, Electric Propulsion Systems Branch, 21000 Brookpark Rd., MS 301-3, AIAA Associate Fellow.

I. Introduction

HALL thrusters are an electric propulsion technology that is becoming an increasingly attractive option for orbit-raising applications as well as NASA science and human exploration missions. Under the sponsorship of the Space Technology Mission Directorate, NASA is seeking to advance the state-of-the-art Hall thruster technology by developing a high-power, high-specific impulse, high-throughput thruster for the Solar Electric Propulsion Technology Demonstration Mission (SEP TDM). This joint development effort between Glenn Research Center (GRC) and the Jet Propulsion Laboratory (JPL) has resulted in the 12.5 kW Hall Effect Rocket with Magnetic Shielding (HERMeS). Numerous tools including thermal models, magnet models, flow models, and plasma models were utilized to design the HERMeS thruster to meet the requirements of potential missions for the SEP TDM, including the Asteroid Redirect Robotic Mission (ARRM).[1-5] Two thrusters have been fabricated to-date, Technology Development Unit (TDU) 1, and TDU2. TDU1 has undergone extensive performance and thermal characterization at NASA GRC, with wear testing planned for the near future.[6, 7] Performance and environmental testing are currently planned for TDU2 at JPL.

Potential missions for the SEP TDM, such as ARRM, place demanding lifetime requirements on the thruster that can exceed 50,000 hours. In order to meet these requirements, magnetic shielding was incorporated into the thruster design. The concept of magnetic shielding was originally explained by JPL as the reason behind the near-zero channel erosion rates observed during the BPT-4000 Qualification Life Test after ~ 5,600 hours of operation.[8, 9] Since then, the concept has been investigated and demonstrated in 6-kW and 20-kW Hall thrusters to significantly reduce channel erosion rates.[10-13] While the reader is encouraged to read the referenced publications for a full understanding of the concept of magnetic shielding, a brief summary of the pertinent details are presented here.

Because electron conductivity is much higher along a magnetic field line compared to across them, electrons can quickly thermally equilibrate along them. Therefore, magnetic field lines can be considered isothermal. While the same reasoning can make magnetic field lines close to equipotentials, variations in the electron density along the line causes electric fields to form that balances the resulting pressure gradient. This phenomenon leads to the concept of a thermalized potential along a field line:

$$\phi_p = \phi_{p,0} + T_e ln\left(\frac{n_e}{n_{e,0}}\right), \tag{1}$$

where ϕ_p is the plasma potential along the field line, $\phi_{p,0}$ is the potential on the field line at channel centerline, T_e is the electron temperature along the field line (constant), n_e is the electron number density along the line, and $n_{e,0}$ is the electron number density on the field line at channel centerline.

Sputter erosion of the channel wall can be a life-limiting mechanism in Hall thrusters. Ions within the channel can bombard the surface at high energies gained by the accelerating electric fields within the channel as well as the Debye sheath formed along the wall surface. The concept of magnetic shielding aims to significantly reduce these ion energies by shaping the channel and magnetic field while utilizing the concepts of thermalized potential and isothermality along field lines. Figure 1 illustrates the concept of magnetic shielding. The magnetic field is shaped around the channel near the thruster exit plane such that a field line runs nearly parallel to the wall (called the "grazing line") and continues into a low electron temperature region deep within the channel near the thruster anode. Because magnetic field lines are isothermal, this configuration will maintain low electron temperatures along the channel walls, minimizing the energy gained by ions in the sheath. Furthermore, based on Eq. (1), because the electron temperature is low, this field line should not deviate greatly from an equipotential line. Therefore, near-anode potentials which exist deep in the

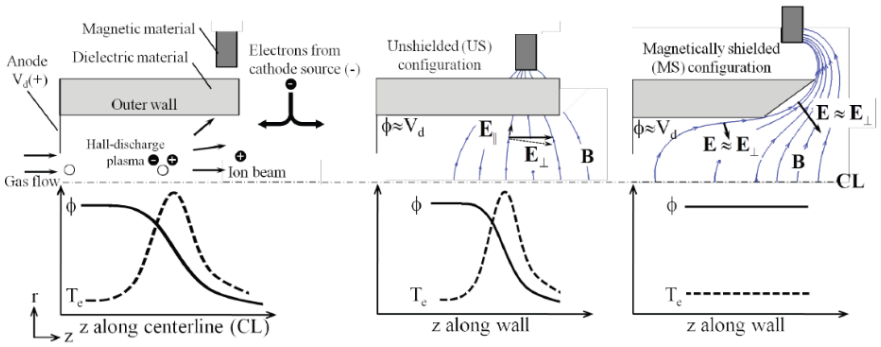

Figure 1. Diagram illustrating the concept of magnetic shielding. By shaping the channel as well as the magnetic field, high plasma potentials and low electron temperatures can be maintained near the channel exit plane. These features will significantly reduce the ion impact energies and consequently the erosion rates at the channel walls. Image taken from Ref. 10.

channel should also be maintained at the channel walls, minimizing or even eliminating the beam energy gained by ions from the accelerating electric field.

In order to characterize the degree of magnetic shielding within HERMeS TDU1, eight Langmuir probes were flush-mounted along each channel wall. Flush-mounted Langmuir probes have been used successfully in the past to measure erosion-relevant properties in Hall thrusters.[10, 13-21] These probes were used to measure the local plasma potential and electron temperature along each wall, with a focus on the exit plane region that is characterized by high erosion rates in unshielded Hall thrusters. The thruster was operated across a wide range of discharge voltages and power levels to characterize the magnetic shielding across the HERMeS throttle table, especially at high specific impulse operation. Parametric studies were also conducted that varied the facility backpressure as well as the magnetic field strength to determine the sensitivity of the magnetic shielding to these factors.

The paper is organized as follows: Section II describes the experimental setup for the investigation, including the vacuum facility, Hall thruster, and flush-mounted Langmuir probes. A description of the test flow, including the sequence of operating conditions tested, is also included at the end of Section II. Section III discusses the measured plasma potentials and electron temperatures at nominal thruster conditions as well as at elevated facility pressures and magnetic field strengths. Finally, Section IV provides a summary and overall conclusions of the investigation.

II. Experimental Apparatus

A. Vacuum Facility

This investigation was conducted in Vacuum Facility 5 (VF-5) at NASA GRC. VF-5 is a 4.6-m-diameter by 18.3-m-long cylindrical vacuum chamber that is equipped with numerous cryogenic surfaces as well as 20 0.8-m-diameter oil diffusion pumps. Facility pressure for this study was monitored by four hot-cathode ionization gauges, three mounted near the thruster and a fourth mounted on the facility wall mid-section.[7] Ionization gauge #2, mounted at approximately 1 o'clock with respect to the thruster when looking upstream, was pointed towards the facility wall and used as the primary gauge in this study (see Fig. 2). A facility base pressure of 3.5×10^{-7} Torr was routinely achieved. For a total xenon flow rate of 30.3 mg/s, the operating pressure was 6.9×10^{-6} Torr, corrected for xenon. This corresponds to the operating condition of 300 V, 9.4 kW, and the facility pressure did not exceed this value during testing except when facility pressure studies were conducted as part of the investigation.

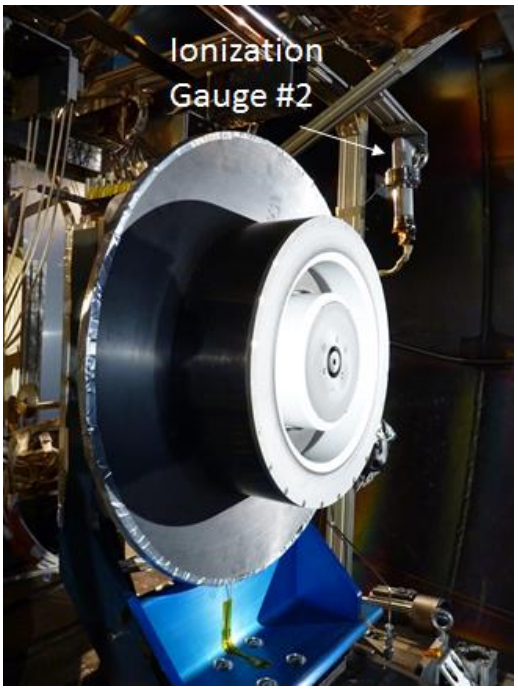

Figure 2. Photograph of the TDU1 Hall thruster within VF-5 at NASA GRC.

B. Hall Thruster

The test article for this study was the HERMeS TDU1 Hall thruster. The HERMeS thruster is a 12.5-kW class, highly throttleable Hall thruster capable of specific impulses up to 3000 s. The thruster has undergone extensive performance and thermal characterizations at NASA GRC within VF-5.[6, 7] For this study, the thruster was placed in the main volume of the facility to assure the lowest possible backpressure conditions were attained during thruster operation. Figure 2 shows a photograph of TDU1 mounted within VF-5 just prior to testing. While the thruster was mounted on a thrust stand for convenience, thrust measurements were not taken during this investigation due to the large amount of probe wires routed from the thruster. The thruster was operated using commercially available power supplies and mass flow controllers, additional details of which can be found in Ref. 7. The cathode flow rate was maintained at 7% of the anode flow rate throughout the study. A symmetric magnetic field topology (one that is symmetric about channel centerline) was used for all operating conditions, and the magnetic field strength was chosen to maximize the anode efficiency as measured by a thrust stand, defined as:

$$\eta_a = \frac{T^2}{2\dot{m}_a P_d}, \tag{2}$$

where η_a is the anode efficiency, T is the measured thrust, $\dot{m}_a$ is the anode mass flow rate, and P_d is the discharge power.

To enable studies involving the facility pressure, an auxiliary flow line was placed within VF-5 at the mid-length of the chamber and pointing downstream of the thruster. This flow line was used to feed additional xenon into the chamber to artificially elevate the backpressure above the nominal, lowest operating pressure. During these studies, the thruster was operated at constant power by adjusting the anode mass flow rate to maintain a constant discharge current. Ionization gauge #2 was used to determine the magnitude of the increase in facility pressure.

C. Langmuir Probe

Eight Langmuir probes were flush-mounted along each channel wall to measure the local plasma properties relevant to erosion and characterization of the magnetic shielding of the wall. Each probe tip was composed of 0.41-mm-diameter pure tungsten wire whose ends were flattened using a diamond file prior to installation. Because each wire was inserted into the channel in the radial direction (except for probe #1, see Fig. 4), probe tips located along the chamfered region of the wall had to be shaped to the angle that corresponds to the chamfer surface. The tungsten wires were approximately 25-40 mm long and interfaced with high-temperature insulated lead wires using pins and sockets. A new discharge channel was fabricated in order to facilitate probe installation. In particular, five slots were machined on the non-plasma side of each channel wall, spaced 60 degrees apart. The slots were spaced fairly evenly around the thruster in order to minimize any local heating caused by a reduced channel wall thickness. These slots provided the necessary space for the probe tips and lead wires to be routed to the back of the thruster.

Given the limited space for diagnostics, the tungsten wires had to be shaped to fit the contour of the channel within the slot. Upstream of the chamfer, this shape resulted in a simple 90 degree bend. However, probes placed along the chamfer required multiple bends in order to properly fit within the slot (see Fig. 3). The probes were held in place using high temperature ceramic paste within holes drilled into the channel wall, and the remaining probe length and lead wires within the slot were potted with identical paste. Once the lead wires were clear of the discharge channel, fiberglass sleeve was used to provide additional protection because the probe wires had to be routed around multiple conducting surfaces before reaching the back of the thruster. After the wires were a sufficient distance from the thruster to avoid large heat loads, they interfaced with shielded coaxial cabling to reduce electromagnetic noise. This cabling comprised the remainder of the electrical line up to the vacuum feedthrough.

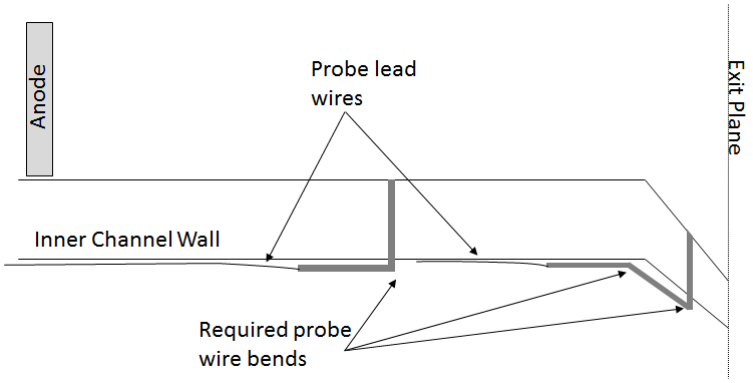

Figure 3. Schematic illustrating how probe wires were bent to fit the contour of the non-plasma side of the channel wall.

Eight probes were placed along each channel wall at various axial distances from the thruster exit plane (see Fig. 4). Probes were placed primarily in the vicinity of the chamfer (probes #2-5) because this region is critical towards the characterization of magnetic shielding. Probe #1 was placed on the channel surface coincident with the thruster exit plane in order to investigate plasma properties that may be responsible for magnetic pole erosion in this region for magnetically shielded Hall thrusters.[22-24] Probes #6-8 were placed further upstream to ensure plasma properties were consistent with magnetic shielding throughout the channel, as well as to investigate the possibility of high plasma densities upstream of the chamfer that were indicated in previous plasma simulations and thruster testing. Due to uncertainties in the probe collection area, trends in plasma density could not be determined with reasonable certainty, and are therefore not reported here.

For convenience, each probe will be referred to using a two-character designation "XY". In this designation, "X" will be "I" if the probe is on the inner wall and "O" if on the outer wall. The second character "Y" corresponds to the

probe number listed in Fig. 4. For example, "I2" refers to probe #2 on the inner wall. Because the primary objective of the investigation was to determine the degree of magnetic shielding, probes I2, I5, O2, and O5 were deemed critical for the characterization. This is because probe #2 is expected to have the lowest plasma potentials and highest electron temperatures within the channel, while the properties at probe #5 are sensitive to the exact shape and location of the "grazing" magnetic field line. Due to their importance, no additional probes were placed within the slots containing probes #2 and #5 in the event of a breakdown in insulation causing probe-to-probe electrical shorting. The outer wall probes were staggered azimuthally from the inner wall probes to avoid any interactions between probes across magnetic field lines.

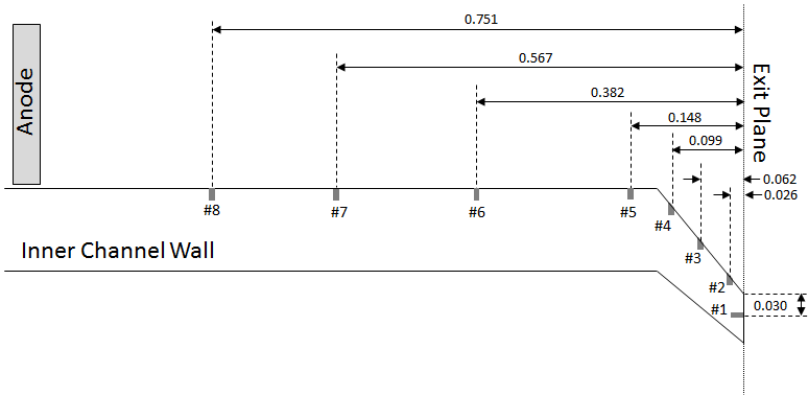

Figure 4. Schematic illustrating the axial location of each Langmuir probe along the inner wall with respect to the thruster exit plane. All values are in units of thruster channel lengths, and probe locations are identical along the outer channel wall. Not to scale.

During operation, each probe was connected to a custom-made circuit box that measured the applied probe voltage as well as the collected current (see Fig. 5). Probe voltage was supplied using a 1000-V, 40-mA bipolar power supply connected to a function generator. A symmetric triangle wave with a frequency of 10 Hz was used to bias each probe. A voltage divider comprised of 10-MΩ and 0.10-MΩ resistors was used to measure the voltage, while the collected current was measured across a 500-Ω, 25-W power resistor. These signals were passed through voltage-following instrumentation amplifiers to reduce zero-drift and amplification noise before being passed through voltage-following isolation amplifiers that protected the data acquisition system (DACS). Blocking diodes were placed across the input signal to the instrumentation amplifiers to protect them from large electrical spikes. Data were collected from the DACS for one second at a scan rate of 10 kHz resulting in 20 I-V characteristics per probe per operating condition, each containing 500 data points.

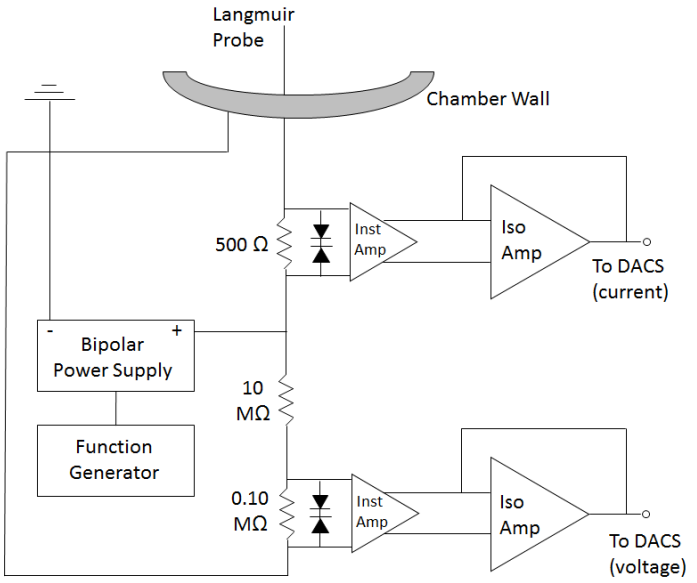

Figure 5. Electrical schematic of the circuit used to measure the applied voltage and collected current from each Langmuir probe.

Data from all 20 I-V characteristics were plotted together and boxcar averaged with a window of 25 points to smooth the data prior to any analysis. Analysis of the data largely follows simple Langmuir probe theory[25, 26] and has been described in a prior publication.[19] During the investigation, certain probes exhibited signs of leakage current, or a low impedance to facility ground. The resulting I-V characteristics appeared to be a superposition of a linear response and the more traditional plasma response of a Langmuir probe (see Fig. 6). These characteristics were corrected by performing linear regression on

the portion of the trace that exhibited a purely linear response, and subtracting out the resulting function. The remaining I-V characteristic was analyzed and produced results similar to adjacent probes that did not exhibit leakage current. Therefore, this corrective technique was deemed acceptable for the purposes of measuring plasma potential and electron temperature. Only a few probes exhibited significant leakage current over the course of the investigation. Probe I2 exhibited leakage current throughout the test, while probe O2 shows signs of leakage current during nominal operation at 300 and 800 V discharge voltage. Probes I3, O3, O4 and O6 all appeared to exhibit signs of leakage current for elevated magnetic field strengths at 300 V, 9.4 kW. This was likely due to the reduced probe current observed at these conditions (see Section III-C for additional discussion of this trend) causing a drop in the plasma-to-leakage current ratio. Probe I3 also exhibited leakage current at elevated discharge voltages of 500 and 600 V. Based on variations of the line fits during analysis of the data, uncertainties in the electron temperature and plasma potential are conservatively estimated as ± 1 eV and ± 5 V, respectively.

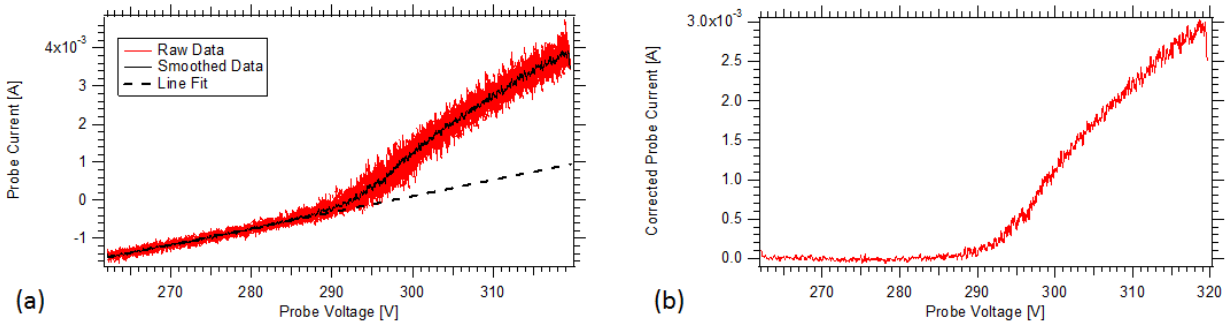

Figure 6. Example of I-V characteristic that exhibited signs of leakage current and the technique used to correct the data. (a) Uncorrected characteristic and the line fit used to estimate the linear behavior of leakage current. (b) Corrected current that exhibits the typical characteristic of a Langmuir probe.

D. Test Flow

The characterization of magnetic shielding on the TDU1 thruster was desired across the entire throttle table, primarily under nominal conditions but also at various facility pressures and magnetic field strengths. However, due to the routing of the probe wires around multiple thruster surfaces, electrical arcing and subsequent probe failure was a risk at elevated discharge voltages where the probes would need to be biased as high as 850 V with respect to facility ground. With this in mind, operating conditions were tested in a sequence that would maximize the data set collected while minimizing risk to the probes, placing importance on characterization at key operating conditions such as 300 V, 9.4 kW. Test termination would occur once all the data were collected at desired conditions, or multiple failures of critical probes made characterizations infeasible. It should be noted that probes O1 and I4 had low impedance to the thruster body prior to testing. These probes were not deemed critical enough to warrant the risk of thruster disassembly and repair, therefore no data are available at these locations. The resulting test flow was as follows:

- Data were collected at 300 V, 4.7 kW under nominal conditions. This operating point was chosen as a relatively benign condition with minimal risk to probes while providing initial magnetic shielding characterization of the thruster. Probe I1 during the initial characterization provided no viable data, and therefore was not used for the remainder of the investigation.
- Data were collected at 300 V, 9.4 kW, as well as 400 and 500 V, 12.5 kW under nominal conditions. Leakage current began occurring on multiple probes and probe I8 failed at 500 V.
- Before testing at higher discharge voltages and risking additional probe failures, data were collected at 300 V, 9.4 kW at elevated facility pressures as well as higher magnetic field strengths in order to characterize the sensitivity of the magnetic shielding to these parameters.
- Data were then collected at 600 V, 12.5 kW under nominal conditions. During operation, probes I6 and O6 experienced failures.
- Data were collected at 700 V, 12.5 kW under nominal conditions. During operation, multiple arcs were observed at the thruster and probes I3, O3, O4, I5, O7, and O8 experienced failures. Despite losing one of the critical probes (I5), it was decided that characterization of magnetic shielding could still be obtained with the remaining probes.
- Data were collected at 800 V, 12.5 kW under nominal conditions. Attempts were made to obtain data at higher magnetic field strengths, but probes O2 and I2 experienced failures. The test was then terminated.

Despite multiple probe failures during the course of the investigation, enough data were collected to characterize the magnetic shielding across the TDU1 throttle table as well as determine its sensitivity to facility pressure and magnetic field strength. The results of these studies are presented in the following section.

III. Results and Discussion

The plasma potential and electron temperature were measured along the TDU1 channel walls under nominal conditions (lowest facility pressure and performance-optimized magnetic field) at 300 V, 4.7 kW; 300 V, 9.4 kW; 400, 500, 600, 700, and 800 V, 12.5 kW. These properties will be presented and discussed in Section III-A. In addition, Section III-B will discuss data collected at 300 V, 9.4 kW at 1X, 2X and 3X facility pressure, where 1X corresponds to the nominal (lowest) operating pressure, 2X corresponds to double that pressure, etc. During these studies, the discharge power was kept constant by adjusting the anode mass flow rate to maintain a constant discharge current. Finally, Section III-C presents and discusses axial profiles of plasma potential and electron temperature at 300 V, 9.4 kW while operating at several magnetic field strengths higher than the optimized strength.

A. Axial Profiles Under Nominal Conditions

Axial profiles of the plasma potential along the channel walls are shown in Fig. 7. All values were adjusted by the cathode-to-ground voltage such that all potentials are reported with respect to cathode potential. At all operating conditions tested, the plasma potential along both walls is within 13 V of the anode potential, even near the thruster exit plane. It is interesting to note that all plasma potentials remain above the anode potential. This may be indicative of the finite sheath potential drop at the anode surface, which would elevate the plasma potential of the ionization region several volts above the anode potential. For certain operating conditions, the plasma potential rises slightly as the exit plane is approached. However, these variations are within measurement uncertainty and therefore may not indicate an actual trend. Regardless, potentials along each channel wall for a given operating condition vary by ≤ 5 V, indicating a minimal amount of beam energy that ions can obtain to sputter erode the channel surface.

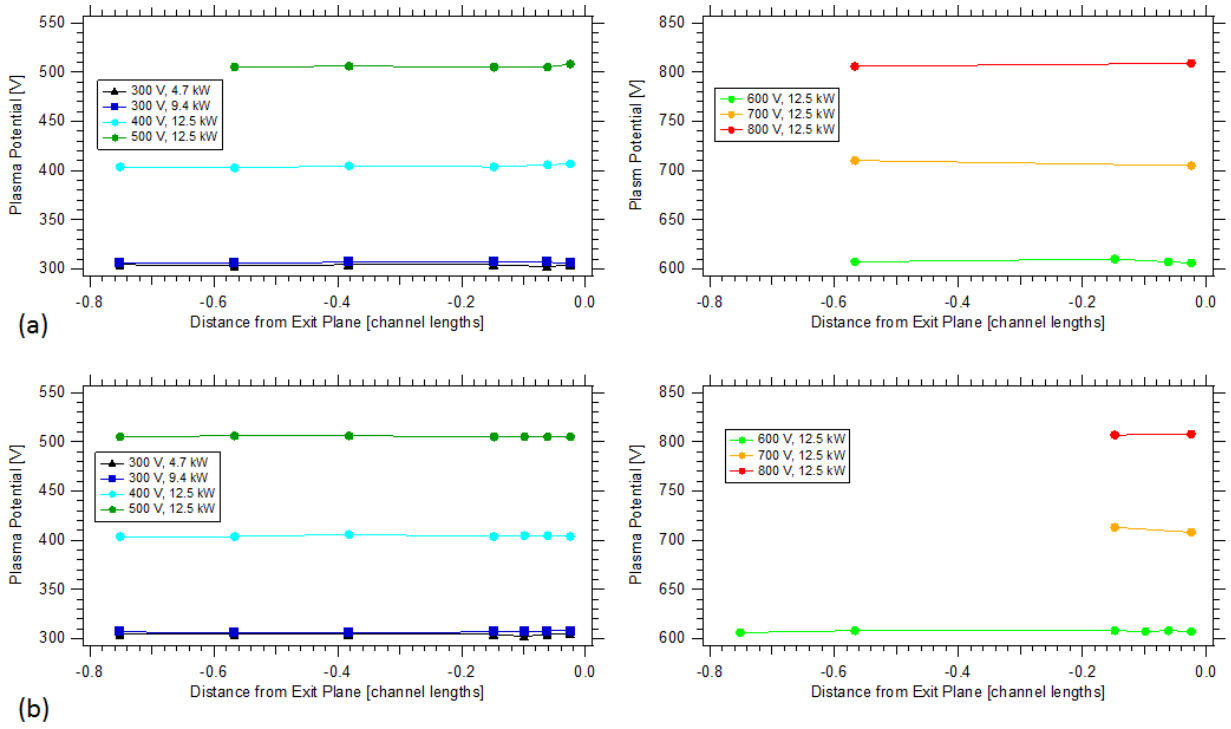

Figure 7. Measured plasma potentials with respect to cathode potential along the (a) inner channel wall and (b) outer channel wall. Estimated uncertainty is ± 5 V.

Figure 8 shows the measured axial profiles of electron temperature along the inner and outer channel walls under nominal conditions. For all conditions tested, the electron temperature remained ≤ 5 eV, even near the thruster exit plane. Under most conditions, a slight rise of 1-2 eV occurs as the exit plane is approached, however the magnitude

of this trend is near the measurement uncertainty. Such low electron temperatures along the channel walls even at discharge voltages as high as 800 V is a major accomplishment of the HERMeS thruster design, in particular of the magnetic field topology. Prior investigations of thrusters that were retrofitted to be magnetically shielded measured reduced electron temperatures near the thruster exit plane compared to unshielded thrusters, but values still approached 10-15 eV.[10, 13] Because HERMeS was initially designed and not merely retrofitted to be magnetically shielded, a more effective magnetic circuit was able to be designed and fabricated.

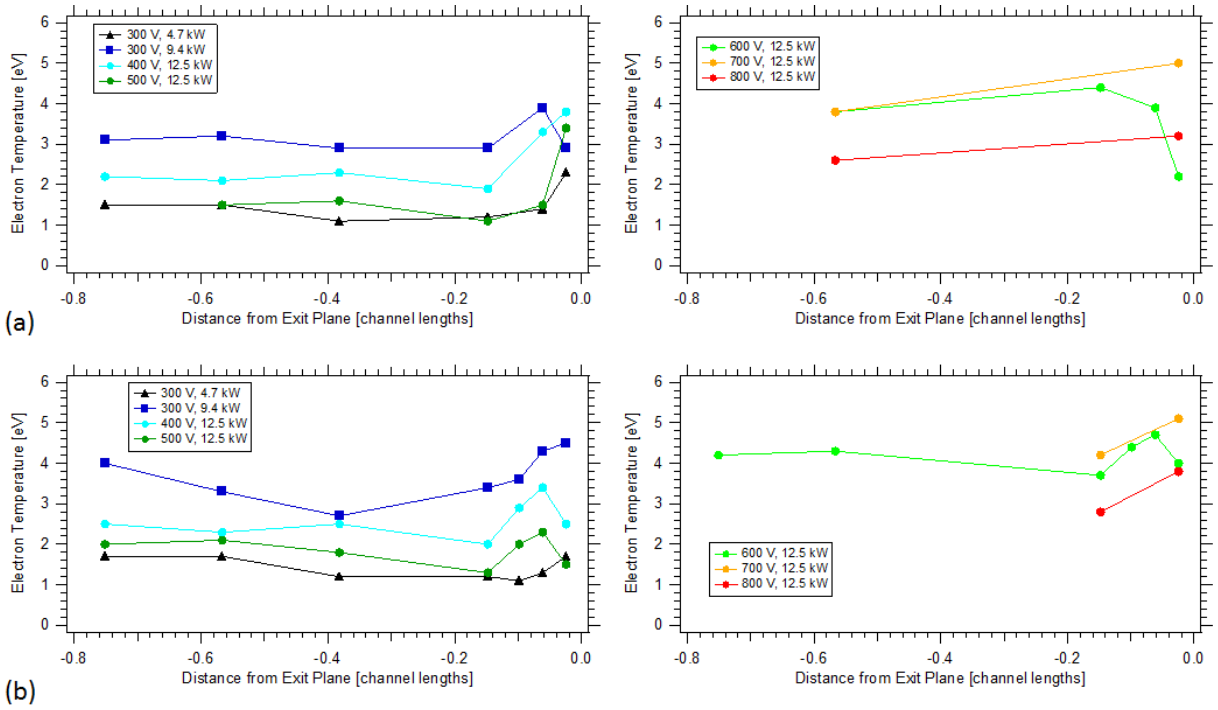

Figure 8. Measured electron temperatures along the (a) inner channel wall and (b) outer channel wall. Estimated uncertainty is ± 1 eV.

The sheath energy gained by ions at the walls can be estimated using the Hobbs and Wesson solution for space-charge-limited emission from a surface.[10, 27] For a xenon plasma with an electron temperature of 5 eV, the sheath potential at a boron nitride surface is 21 V. Based on results from Fig. 7, the maximum beam energy gained based on the measured plasma potentials is 5 eV. Therefore, in the HERMeS thruster the largest impact energy that singly-charged ions can obtain is 26 eV. Based on comparisons between simulation and experiment for the H6 Hall thruster channel wall erosion rates, the threshold ion energy for boron nitride sputtering is estimated to be 40 ± 5 eV.[12] This indicates that singly-charged ions are unable to sputter erode the channel in HERMeS even at the thruster exit plane. While multiply-charged species will exceed the threshold energy for sputtering, the overall low impact energies and the reduced densities of particles capable of sputtering will significantly reduce the overall erosion rates even at high specific impulse operation.

B. Axial Profiles at Various Facility Backpressures

Figure 9 provides the axial profiles of the measured plasma potential and electron temperature along the inner and outer channel walls as a function of facility backpressure at 300 V, 9.4 kW. It is evident from the figure that no significant changes were observed as the facility pressure was elevated. Magnetic shielding was effectively maintained at all facility pressures tested. Measured electron temperatures do indicate a slight increase at all locations with increasing facility pressure. Previous investigations in other thrusters have observed that the acceleration zone and plasma recede further into the channel towards the anode with elevated facility pressure.[19, 28-32] In particular, this shift was observed to cause increased electron temperatures along the channel walls of the HiVHAc Hall thruster.[19] It is possible that a similar shift in the plasma is occurring towards the anode, resulting in slightly elevated temperatures at higher pressure. However, the magnetically shielded configuration as well as HERMeS's centrally-mounted cathode likely make the properties at the channel wall more insensitive to facility pressure.[2, 7, 33] Regardless, the

change in electron temperature is within the measurement uncertainty, and the data indicate that the effectiveness of magnetic shielding will only improve at lower pressures, e.g. flight conditions.

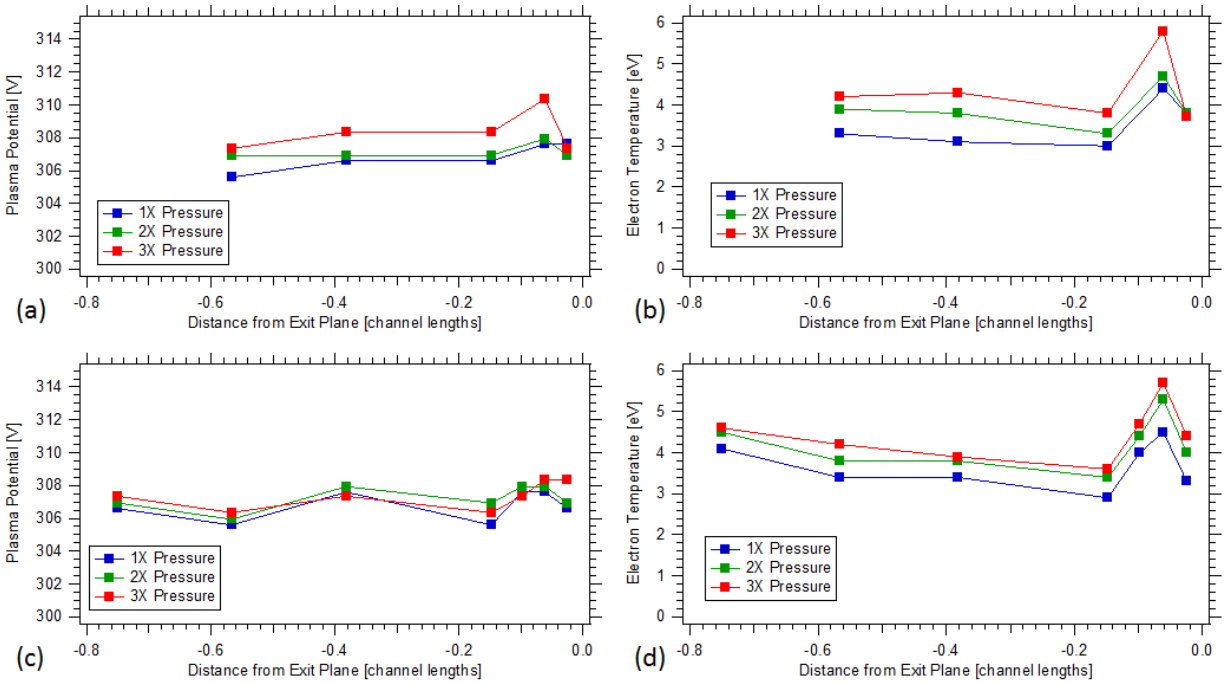

Figure 9. Measured plasma properties along the channel walls at 300 V, 9.4 kW for various facility pressures. (a) Plasma potential and (b) electron temperature along the inner channel wall. (c) Plasma potential and (d) electron temperature along the outer channel wall. Estimated uncertainties for plasma potential and electron temperature are ± 5 V and ± 1 eV, respectively.

C. Axial Profiles at Various Magnetic Field Strengths

Figure 10 shows the measured plasma potential and electron temperature along the inner and outer channel walls for various magnetic field strengths at 300 V, 9.4 kW. Values of the peak magnetic field along channel centerline have been normalized by the nominal value that optimizes performance. As with variations in facility pressure, no significant changes were observed over the range of magnetic fields tested. However, the local plasma potentials appeared to drop by approximately 5-10 V by increasing the magnetic field strength by 2.5X. This is correlated to a drop in electron temperature of approximately 1-2 eV, primarily upstream of the chamfer. Despite the drop in plasma potential, variations along the channel wall for a given magnetic field setting remain ≤ 5 V. Coupled with the drop in electron temperature, magnetic shielding appears to be slightly more effective at higher magnetic field settings. However, these trends are once again within the measurement uncertainty.

While the plasma potential and electron temperature did not change significantly, the collected current at the probes was found to decrease with increasing magnetic field strength. To illustrate this, the ion saturation current is plotted as a function of the relative field strength for the critical probe #5 on the inner and outer channel walls. While the uncertainty in probe area prevents accurate determination of the ion number density, relative changes in the collected ion current can still provide information on how the number density at a given location is changing across operating conditions. Figure 11 shows that an increase of 2.5X in the magnetic field strength can cause a decrease in ion current of nearly 50% on the inner wall and over 80% on the outer wall. Furthermore, negligible changes are observed in the ion current above 1.7X field strength along the inner wall, while significant changes continue to occur along the outer wall over the full range of tested field strengths. Therefore, while the plasma potential and electron temperature are not significantly affected by increased field strength, erosion rates may be reduced even further at higher magnetic fields through a reduced local plasma density, especially along the outer channel wall.

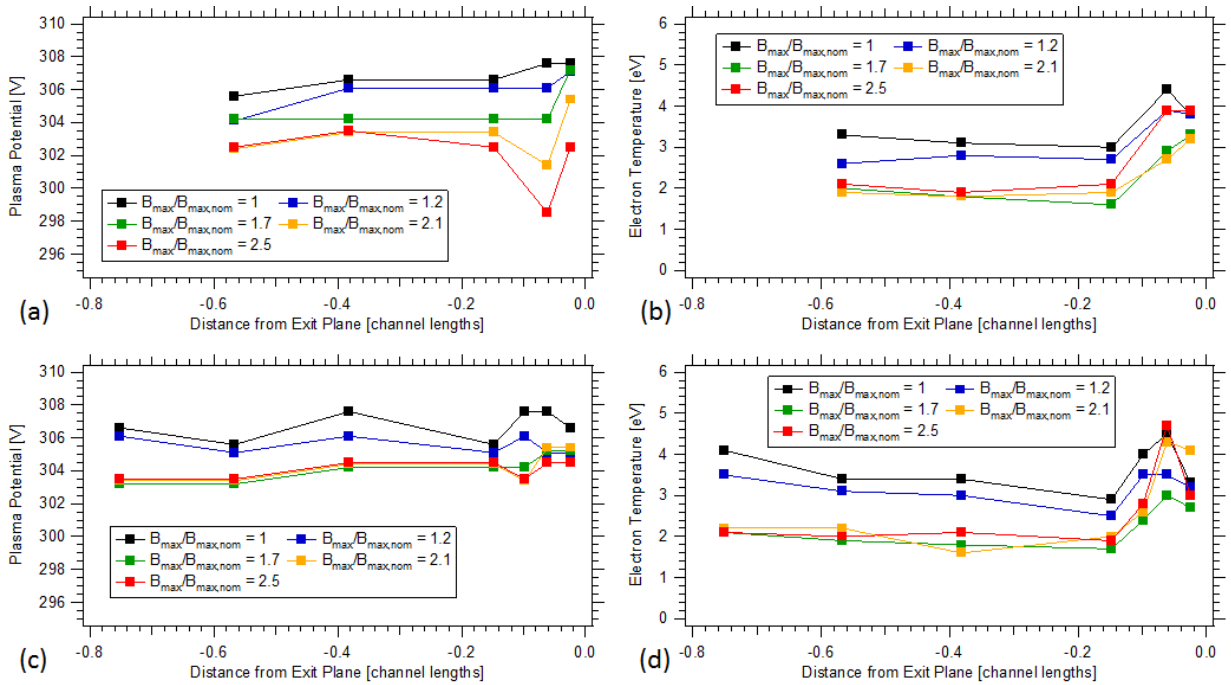

Figure 10. Measured plasma properties along the channel walls at 300 V, 9.4 kW for various magnetic field strengths. (a) Plasma potential and (b) electron temperature along the inner channel wall. (c) Plasma potential and (d) electron temperature along the outer channel wall. Estimated uncertainties for plasma potential and electron temperature are ± 5 V and ± 1 eV, respectively.

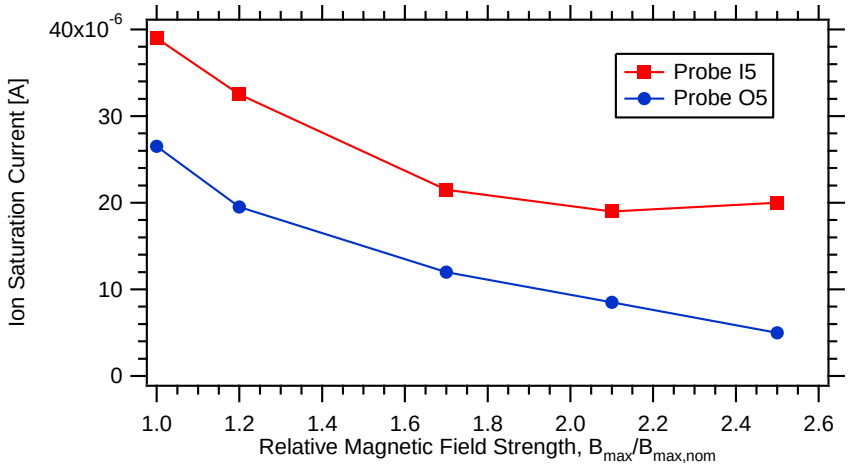

Figure 11. Measured ion saturation current for the critical probes I5 and O5 as a function of the relative magnetic field strength at 300 V, 9.4 kW.

IV. Conclusions

In order to characterize the degree of magnetic shielding within the HERMeS TDU1 thruster, eight Langmuir probes were flush-mounted at various axial locations within each channel wall. The measured plasma potentials and electron temperatures were found to be consistent with a magnetically shielded thruster at all operating conditions tested, even at 800 V discharge voltage. Under nominal conditions (lowest facility pressure and optimized magnetic field strength), the measured plasma potentials (with respect to cathode potential) were all within 13 V of the anode potential, with variations along each wall being ≤ 5 V. Electron temperatures were maintained at ≤ 5 eV, even near the thruster exit plane at elevated discharge voltages. Resulting ion energies at the wall appear to be below the threshold energy for sputtering of boron nitride, indicating that singly-charged xenon is unable to sputter erode the

channel wall in the TDU1. Parametric studies indicate that the plasma properties along the channel wall are fairly insensitive to facility backpressure, with the thruster remaining well shielded at pressures 3X higher than nominal conditions. Measurements at elevated magnetic field strengths indicate that while the plasma potential and electron temperature are not strongly affected, significant reductions in plasma density near the walls can be obtained at field strengths 1.7-2.5X higher than the optimized value. Overall, the HERMeS thruster exhibits a high degree of magnetic shielding along the channel walls, thereby mitigating discharge channel erosion as a life-limiting mechanism.

Acknowledgments

The authors would like to thank and acknowledge the Space Technology Mission Directorate (STMD) for funding this work as well as Mike Barrett for serving as the Project Manager. The authors would like to thank and acknowledge the many members of the HERMeS team, including Dan Herman, Rich Hofer, Jay Polk, Mike Sekerak, and George Williams, who provided input while troubleshooting issues as well as aid during thruster installation and facility pumpdown. The authors would also like to thank and acknowledge Kevin Blake, George Jacynycz, Terry Jansen, and Drew Fausnaugh for providing facility support and helping with thruster installation during this investigation. Extra thanks go to Kevin Blake for having the extreme skill and patience to drill 16 tiny holes into the discharge channel and then route 16 probe wires out the back of the thruster.

References

[1]Herman, D. A., et al., "The Development of the Ion Propulsion System for the Solar Electric Propulsion Technology Demonstration Mission", *34th International Electric Propulsion Conference*, IEPC-2015-008, Hyogo-Kobe, Japan, July 4-10, 2015.

[2]Hofer, R. R., Herman, D. A., Polk, J. E., Kamhawi, H., and Mikellides, I. G., "Development Approach and Status of the 12.5 kW HERMeS Hall Thruster for the Solar Electric Propulsion Technology Demonstration Mission", *34th International Electric Propulsion Conference*, IEPC-2015-186, Hyogo-Kobe, Japan, July 4-10, 2015.

[3]Huang, W., Yim, J. T., and Kamhawi, H., "Design and Empirical Assessment of the HERMeS Hall Thruster Propellant Manifold", *62nd JANNAF Propulsion Meeting*, JANNAF-2015-3926, Nashville, TN, June 1-5, 2015.

[4]Mikellides, I. G., et al., "Hall2de Simulations of a 12.5-kW Magnetically Shielded Hall Thruster for the NASA Solar Electric Propulsion Technology Demonstration Mission", *34th International Electric Propulsion Conference*, IEPC-2015-254, Hyogo-Kobe, Japan, July 4-10, 2015.

[5]Yim, J. T. and Huang, W., "Flow Analysis and Modeling of the HERMeS Hall Thruster Propellant Manifold", *62nd JANNAF Propulsion Meeting*, JANNAF-2015-3884, Nashville, TN, June 1-5, 2015.

[6]Huang, W., Kamhawi, H., Myers, J. L., Yim, J. T., and Neff, G., "Non-Contact Thermal Characterization of NASA's 12.5-kW Hall Thruster", *51st AIAA/SAE/ASEE Joint Propulsion Conference*, AIAA-2015-XXXX, Orlando, FL, July 27-29, 2015.

[7]Kamhawi, H., et al., "Performance Characterization of the Solar Electric Propulsion Technology Demonstration Mission 12.5-kW Hall Thruster", *34th International Electric Propulsion Conference*, IEPC-2015-007, Hyogo-Kobe, Japan, July 4-10, 2015.

[8]de Grys, K., Mathers, A., Welander, B., and Khayms, V., "Demonstration of 10,400 Hours of Operation on a 4.5 kW Qualification Model Hall Thruster", *46th AIAA/ASME/SAE/ASEE Joint Propulsion Conference and Exhibit*, AIAA-2010-6698, Nashville, TN, July 25-28, 2010.

[9]Mikellides, I. G., et al., "Magnetic Shielding of the Acceleration Channel Walls in a Long-Life Hall Thruster", *46th AIAA/ASME/SAE/ASEE Joint Propulsion Conference and Exhibit*, AIAA-2010-6942, Nashville, TN, July 25 - 28, 2010.

[10]Hofer, R. R., Goebel, D. M., Mikellides, I. G., and Katz, I., "Design of a Laboratory Hall Thruster with Magnetically Shielded Channel Walls, Phase II: Experiments", *48th AIAA/ASME/SAE/ASEE Joint Propulsion Conference and Exhibit*, AIAA-2012-3788, Atlanta, Georgia, July 30 - August 1, 2012.

[11]Mikellides, I. G., Katz, I., and Hofer, R. R., "Design of a Laboratory Hall Thruster with Magnetically Shielded Channel Walls, Phase I: Numerical Simulations", *47th AIAA/ASME/SAE/ASEE Joint Propulsion Conference and Exhibit*, AIAA-2011-5809, San Diego, CA, July 31 - August 3, 2011.

[12]Mikellides, I. G., Katz, I., Hofer, R. R., and Goebel, D. M., "Design of a Laboratory Hall Thruster with Magnetically Shielded Channel Walls, Phase III: Comparison of Theory with Experiment", *48th AIAA/ASME/SAE/ASEE Joint Propulsion Conference and Exhibit*, AIAA-2012-3789, Atlanta, GA, July 30 - August 1, 2012.

[13]Shastry, R., Huang, W., Haag, T. W., and Kamhawi, H., "Langmuir Probe Measurements within the Discharge Channel of the 20-kW NASA-300M and NASA-300MS Hall Thrusters", *33rd International Electric Propulsion Conference*, IEPC-2013-122, Washington, D.C., October 6-10, 2013.

[14]Arkhipov, A. S., Kim, V., Sidorenko, E. K., and Khartov, S. A., "Analysis of Energy Balance in the Discharge of SPT Using Results of Its Integral Parameters and Plume Characteristics Measurements", *31st International Electric Propulsion Conference*, IEPC-2009-097, Ann Arbor, MI, September 20 - 24, 2009.

[15]Azziz, Y., Warner, N. Z., Martinez-Sanchez, M., and Szabo, J. J., "High Voltage Plume Measurements and Internal Probing of the BHT-1000 Hall Thruster", *40th AIAA/ASME/SAE/ASEE Joint Propulsion Conference and Exhibit*, AIAA-2004-4097, Fort Lauderdale, FL, July 11-14, 2004.

[16]Kim, V., et al., "Local Plasma Parameter Measurements by Nearwall Probes Inside the SPT Accelerating Channel Under Thruster Operation with Kr", *38th AIAA/ASME/SAE/ASEE Joint Propulsion Conference and Exhibit*, AIAA-2002-4108, Indianapolis, IN, July 7-10, 2002.
[17]Shastry, R., "Experimental Characterization of the Near-Wall Region in Hall Thrusters and its Implications on Performance and Lifetime", Ph.D. Dissertation, Aerospace Engineering, The University of Michigan, Ann Arbor, 2011.
[18]Shastry, R., Gallimore, A. D., and Hofer, R. R., "Experimental Characterization of the Near-Wall Plasma in a 6-kW Hall Thruster and Comparison to Simulation", *47th AIAA/ASME/SAE/ASEE Joint Propulsion Conference and Exhibit*, AIAA-2011-5589, San Diego, CA, July 31 - August 3, 2011.
[19]Shastry, R., Kamhawi, H., Huang, W., and Haag, T. W., "Experimental Investigation of the Near-Wall Region in the NASA HiVHAc EDU2 Hall Thruster", *34th International Electric Propulsion Conference*, IEPC-2015-246, Hyogo-Kobe, Japan, July 4-10, 2015.
[20]Szabo, J. J., Warner, N. Z., and Martinez-Sanchez, M., "Instrumentation and Modeling of a High Isp Hall Thruster", *38th AIAA/ASME/SAE/ASEE Joint Propulsion Conference and Exhibit*, AIAA-2002-4248, Indianapolis, IN, July 7-10, 2002.
[21]Warner, N. Z., "Performance Testing and Internal Probe Measurements of a High Specific Impulse Hall Thruster", Ph.D. Dissertation, Aeronautics and Astronautics, Massachusetts Institute of Technology, Cambridge, MA, 2003.
[22]Goebel, D. M., Jorns, B. A., Hofer, R. R., Mikellides, I. G., and Katz, I., "Pole-piece Interactions with the Plasma in a Magnetically Shielded Hall Thruster", *50th AIAA/ASME/SAE/ASEE Joint Propulsion Conference*, AIAA-2014-3899, Cleveland, OH, July 28-30, 2014.
[23]Lopez Ortega, A., Mikellides, I. G., and Katz, I., "Hall2de Numerical Simulations for the Assessment of Pole Erosion in a Magnetically Shielded Hall Thruster", *34th International Electric Propulsion Conference*, IEPC-2015-249, Hyogo-Kobe, Japan, July 4-10, 2015.
[24]Mikellides, I. G. and Ortega, A. L., "Assessment of Pole Erosion in a Magnetically Shielded Hall Thruster", *50th AIAA/ASME/SAE/ASEE Joint Propulsion Conference*, AIAA-2014-3897, Cleveland, OH, July 28-30, 2014.
[25]Hershkowitz, N., *How Langmuir Probes Work*, in *Plasma Diagnostics: Discharge Parameters and Chemistry*, Ch. 3, D.L. Flamm, Editor, Academic Press, Inc., 1989, pp. 113-181.
[26]Lieberman, M. A. and Lichtenberg, A. J., *Principles of Plasma Discharges and Materials Processing*, Second ed., John Wiley & Sons, Inc., Hoboken, NJ, 2005, 757.
[27]Hobbs, G. D. and Wesson, J. A., "Heat flow through a Langmuir sheath in the presence of electron emission", *Plasma Physics*, Vol. 9, 1967, pp. 85-87.
[28]E, P., Yu, D., and Jiang, B., "Experimental Investigation of Backpressure Effects on the Ionization and Acceleration Processes in a Hall Thruster", *31st International Electric Propulsion Conference*, IEPC-2009-119, Ann Arbor, MI, September 20-24, 2009.
[29]Huang, W., Kamhawi, H., and Haag, T., "Effect of Background Pressure on the Performance and Plume of the HiVHAc Hall Thruster", *33rd International Electric Propulsion Conference*, IEPC-2013-058, Washington, D.C., October 6-10, 2013.
[30]Kamhawi, H., Huang, W., Haag, T., and Spektor, R., "Investigation of the Effects of Facility Background Pressure on the Performance and Voltage-Current Characteristics of the High Voltage Hall Accelerator", *50th AIAA/ASME/SAE/ASEE Joint Propulsion Conference*, AIAA-2014-3707, Cleveland, OH, July 28-30, 2014.
[31]Mazouffre, S., Pagnon, D., and Bonnet, J., "Two ways to evaluate the Xe+ ion flow velocity in a Hall effect thruster - LIF spectroscopy and Fabry-Perot interferometry", *40th AIAA/ASME/SAE/ASEE Joint Propulsion Conference and Exhibit*, AIAA-2004-3949, Fort Lauderdale, FL, July 11-14, 2004.
[32]Nakles, M. R. and Hargus, W. A., "Background Pressure Effects on Ion Velocity Distribution Within a Medium-Power Hall Thruster", *Journal of Propulsion and Power*, Vol. 27, No. 4, doi:10.2514/1.48027, July-August, 2011, pp. 737-743.
[33]Kamhawi, H., Haag, T. W., Huang, W., and Hofer, R. R., "The Voltage-Current Characteristics of the 12.5 kW Hall Effect Rocket with Magnetic Shielding at Different Background Pressure Conditions", *62nd JANNAF Propulsion Meeting*, JANNAF-2015-XXXX, Nashville, TN, June 1-5, 2015.